

Journal of Materials Chemistry C

Accepted Manuscript



This is an *Accepted Manuscript*, which has been through the Royal Society of Chemistry peer review process and has been accepted for publication.

Accepted Manuscripts are published online shortly after acceptance, before technical editing, formatting and proof reading. Using this free service, authors can make their results available to the community, in citable form, before we publish the edited article. We will replace this *Accepted Manuscript* with the edited and formatted *Advance Article* as soon as it is available.

You can find more information about *Accepted Manuscripts* in the [Information for Authors](#).

Please note that technical editing may introduce minor changes to the text and/or graphics, which may alter content. The journal's standard [Terms & Conditions](#) and the [Ethical guidelines](#) still apply. In no event shall the Royal Society of Chemistry be held responsible for any errors or omissions in this *Accepted Manuscript* or any consequences arising from the use of any information it contains.

ARTICLE

Fluorescent Aggregates of Hetero-oligophenylene Derivative as “No Quenching” Probe for Detection of Picric Acid at Femtogram Level

Cite this: DOI: 10.1039/x0xx00000x

Received 00th January 2012,
Accepted 00th January 2012

DOI: 10.1039/x0xx00000x

www.rsc.org/

Sharanjeet Kaur, Vandana Bhalla,* Varun Vij and Manoj Kumar*

Abstract: Fluorescent aggregates of hetero-oligophenylene derivative **3** serve as “no quenching” probe for the detection of picric acid (PA) in aqueous media. Photoinduced intermolecular excited state proton transfer from PA to pyridyl nitrogen results in the formation of protonated species which exhibit emission at different wavelength, hence, “no quenching” detection of PA in aqueous media.

Introduction

Among various nitroaromatics, picric acid (PA) is a health hazard as it can cause skin/eye irritation and can affect the organs involved in respiratory system.^{1,2} PA is a strong organic acid,³ and its vapors are hazardous and cause headache, weakness, anemia and liver injury.⁴ Furthermore, with the electron deficient character, the degradation of PA is more difficult in the biosystem, which is probably responsible for many chronic diseases such as sycolosis and cancer.⁵ PA is also used in dye industries, pharmaceuticals, and chemical laboratories.^{6,7} Like many polynitrated aromatic compounds, it is a powerful explosive and its explosive nature is equivalent to 105% of trinitrotoluene (TNT).^{8,9} Further, because of its high solubility in water, it can easily contaminate soil and groundwater when exposed. As a result, there have been considerable efforts for developments of cost efficient, selective,^{10,11} sensitive, fast and portable detection methods for PA in aqueous media.¹²⁻¹⁵ Thus, a variety of fluorescent materials have been developed that serve as turn off sensors for PA.¹⁶⁻²² However, fluorescent sensors showing no quenching response are attractive due to less interference from fluctuation of background fluorescence²³ but fluorescent materials showing no quenching response towards nitroaromatics are still in their infancy.^{24,25} Motivated by better sensitivity and reliability of “no quenching” sensors, we were interested in the development of fluorescent assemblies showing ‘no quenching’ response towards PA.

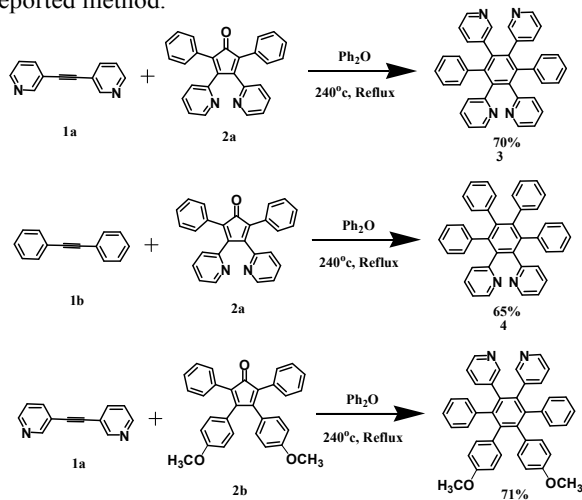
Recently, stimuli responsive smart materials with tunable photophysical properties have attracted considerable research interest.²⁶ Keeping this in view, we designed and synthesized hetero-oligophenylene derivative **3** having pyridine groups for the sensitive detection of PA. Pyridine exhibits Lewis basicity and is good proton acceptor. On the other hand, electron

deficient PA has acidic character. We envisaged that formation of protonated species due to intermolecular transfer of proton from PA to the pyridine group of derivative **3** could influence the photophysical properties of the system. Interestingly, derivative **3** forms fluorescent aggregates in aqueous media and exhibits reversible photoinduced intermolecular excited state proton transfer from PA to pyridine nitrogen of aggregates of derivative **3** and subsequent formation of protonated species exhibited emission at different wavelength, hence, “no quenching” response towards PA was observed in aqueous media. The fluorescent aggregates of derivative **3** serve as better probe for detection of PA in comparison to the previously reported chemosensors for PA.²⁷ To the best of our knowledge, this is the first report where fluorescent aggregates of hetero-oligophenylene derivative **3** serve as “no quenching” chemosensor for PA based on photoinduced intermolecular excited state proton transfer mechanism with a detection limit in the femtogram level.

Results and Discussion

The target compound **3** was synthesized by Diels-Alder reaction of 3-(2-(pyridine-3-yl)ethynyl)pyridine **1a**²⁸ with 2,5-diphenyl-3,4-di(pyridin-2-yl)cyclopenta-2,4-dienone **2a**²⁹ in diphenylether at 240 °C in 70% yield (Scheme 1). The ¹H NMR spectrum of compound **3** showed five doublets at 8.16, 8.12, 7.24, 7.17 and 7.02 ppm, one singlet at 8.08 ppm, one multiplet at 6.83-6.91 ppm and one triplet at 6.8 ppm corresponding to aromatic protons. A parent ion peak for (M + H⁺) was observed at m/z 539.2302 in ESI mass spectrum (pS15 to S17 in ESI⁺). These spectroscopic data corroborate the structure **3** for this compound. To get insight into the role played by 3-pyridyl/2-pyridyl groups in the “no quenching” response, we also synthesized hetero-oligophenylene derivatives **4** and **5**²⁸ as

model compounds incorporating 2-pyridyl and 3-pyridyl groups, respectively. The derivative **4** was synthesized by Diels-Alder reaction of 1,2-diphenylethyne **1b**³⁰ with 2,5-diphenyl-3,4-di(pyridin-2-yl)cyclopenta-2,4-dienone **2a**²⁹ in diphenylether at 240 °C in 65% yield (Scheme 1). The ¹H NMR spectrum of compound **4** showed two doublets at 8.13 and 6.98 ppm, one triplet at 7.19 ppm and one multiplet at 6.73-6.86 ppm corresponding to aromatic protons. A parent ion peak for (M + H⁺) was observed at m/z 537.2332 in ESI mass spectrum (pS18 to S20 in ESI†). The derivative **5** was prepared by reported method.²⁸



Scheme 1. Synthesis of compounds **3** – **5**.

The UV-vis spectrum of compound **3** in EtOH exhibits an absorption band at 213 nm with two shoulders at 245 nm and 271 nm (Figure 1A). On addition of water (60 % volume fractions) to the EtOH solution of derivative **3**, the absorption band at 213 nm is slightly red shifted to 220 nm and a well defined absorption band appeared at 271 nm. The red shifting of the absorption band indicates aggregation of derivative **3** to produce *J*-type assemblies.^{31,32} Since it is known that deaggregation takes place on increasing the temperature,³³ so we carried out temperature dependent UV-vis studies of derivative **3** in H₂O:EtOH (6:4) and it was observed that with increase in temperature up to 70 °C, the absorption band at 220 nm blue shifted to 213 nm (Fig. S1 in ESI†). This revival of absorption band at 213 nm clearly indicates the deaggregation of *J*-type assemblies. To further prove the formation of *J*-assemblies, we carried out concentration dependent ¹H NMR studies of derivative **3** in CDCl₃ (Fig. S2 in ESI†). These studies show the upfield shifting of signals corresponding to aromatic protons. Such an upfield shift is attributed to the intermolecular shielding from the neighboring aromatic molecules, suggesting their tendency to undergo self-association to form aggregates.³⁴ The scanning electron microscopy (SEM) image of compound **3** in the solvent mixture of H₂O:EtOH (6:4) shows the presence of aggregates {Figure 1B (i)}. The solution of aggregates is visibly transparent and stable at room temperature for several weeks.

Derivative **3** in H₂O:EtOH (6:4) exhibits fluorescence emission at 339 nm ($\Phi_F = 0.35$)³⁵ when excited at 273 nm (Figure 1C). The strong emission of aggregates of derivative **3** prompted us to explore

their potential application as chemosensor for the detection of nitro derivatives such as trinitrotoluene (TNT), trinitrobenzene (TNB), picric acid (PA) etc. Thus, we carried out the fluorescence titrations of aggregates of compound **3** in H₂O:EtOH (6:4) toward various nitro derivatives such as picric acid (PA), 2,4,6-trinitrotoluene (TNT), 2,4-dinitrotoluene (DNT), 1,4-dinitrobenzene (DNB), 1,4-benzoquinone (BQ), nitromethane (NM), 2-nitrotoluene (NT). Upon addition of PA up to 2.5 eq to the solution of derivative **3** in H₂O:EtOH (6:4) mixture, the intensity of emission band at 339 nm decreased gradually and a new band appeared at 446 nm (Figure 1C). On addition of PA up to 4 eq the intensity of emission band at 339 nm quenched completely (Inset, Figure 1D) and the intensity of emission band at 446 nm increased (Figure 1D). On further addition of PA up to 7 eq the intensity of emission band at 446 nm increased along with a red shift of 14 nm to give final emission at 460 nm (Figure 1D). The formation of new band at 460 nm suggests the formation of protonated species due to excited state intermolecular proton transfer from PA to pyridyl nitrogen. The factor responsible for this transfer is matching of acidity of phenolic group of PA and basicity of pyridine group in excited state.

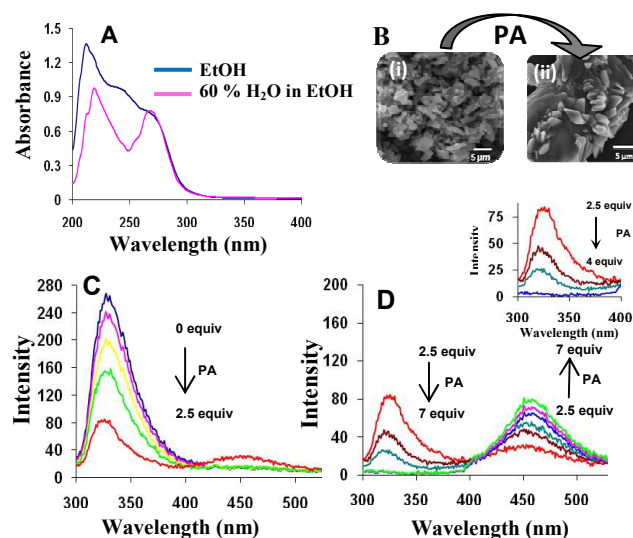


Figure 1. (A) UV-vis absorption spectra of **3** (50 μM) in EtOH and H₂O:EtOH (6:4) buffered with HEPES, pH = 7.0. (B) (i) The scanning electron microscopy (SEM) image of aggregates of compound **3** (10⁻⁴ M) in H₂O:EtOH (6:4) buffered with HEPES, pH = 7.0. (ii) The Scanning electronic microscopy (SEM) image of derivative **3** (10⁻⁴ M) in presence of 7 equivalents of PA in H₂O:EtOH (6:4) buffered with HEPES pH = 7. (C) Fluorescence emission spectra of **3** (50 μM) with the addition of Picric Acid (125 μM) in H₂O:EtOH (6:4) buffered with HEPES, pH = 7.0; λ_{ex} = 273 nm. (D) Fluorescence emission spectra of derivative **3** (50 μM) up to the addition of 350 μM of PA in H₂O:EtOH (6:4) buffered with HEPES pH = 7; λ_{ex} = 273 nm. Inset shows the emission band at 339 nm completely quenched with the addition of 200 μM of PA.

On the other hand the absorption studies of the aggregates of derivative **3** in presence of PA do not suggest the formation of protonated species in the ground state (Fig. S3 in ESI†). The absorption studies of aggregates of derivative **3** in the presence of 7 eq of PA show appearance of a band at 356 nm corresponding to PA (Fig. S4 in ESI†) and increase in absorption intensity of the band at 218 nm whereas slight change in the intensity of absorption band at 273 nm is

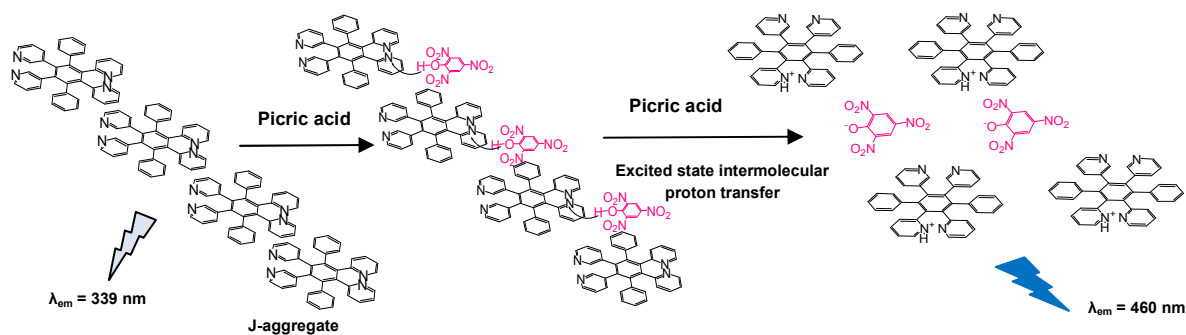


Figure 2. Mechanism of the recognition behavior of aggregates of **3** towards picric acid in H₂O:EtOH (6:4).

observed (Fig. S3 in ESI†). However, the fluorescence spectrum of same solution shows the formation of new band at 460 nm (Fig. S5 in ESI†). Thus, the absorption studies rule out the charge transfer interactions between aggregates of derivative **3** and PA in the ground state. On the basis of fluorescence studies of aggregates of **3** in presence of PA, we propose that sensing mechanism involves two steps (Figure 2). In the first step, interaction between the aggregates of **3** and PA takes place which is responsible for quenching of emission band at 339 nm (Figure 1C and inset Figure 1D). In the next step, we believe that upon light absorption, basicity of pyridyl nitrogen is enhanced³⁶ which facilitates the transfer of proton from PA to pyridyl nitrogen in the excited state. This excited state intermolecular proton transfer from PA to pyridine groups lead to formation of protonated species which is responsible for appearance of new band at 460 nm (Figure 1D). Further, we determined the pK_a of picric acid in H₂O:EtOH (6:4) solution buffered with HEPES at pH = 7, using UV-vis spectroscopic method^{37,38} and it comes out to be 6.45 (Fig. S6 and PS6 in ESI†). This result shows the presence of significant portion of picric acid in its conjugate acid form, hence, supports the proposed mechanism. Further to support our mechanism, we also carried out absorption and emission studies of derivative **3** in acetonitrile with PA (the pK_a of PA in acetonitrile is 11)³⁹ and similar absorption and emission results were obtained which suggest the formation of protonated species due to excited state intermolecular proton transfer from PA to pyridyl nitrogen (Fig. S8 in ESI†). Further, we recorded the ¹H NMR spectrum of derivative **3** in solvent mixture of D₂O:CD₃OD (6:4) in presence of PA which shows average downfield shift of 0.05 ppm in signals corresponding to aromatic protons (Fig. S9 in ESI†). This very low downfield shift in the signal corresponding to aromatic protons indicates the very little charge transfer interaction between derivative **3** and PA. However, the considerable spectral overlap between emission spectrum of aggregates of derivative **3** and absorption spectrum of PA indicates the possibility of energy transfer between aggregates and molecules of PA (Fig. S10 in ESI†). Thus the quenching of emission band at 339 nm is due to energy transfer and very little charge transfer interaction between aggregates of derivative **3** and PA. To confirm the excited state intermolecular proton transfer, we carried out fluorescence studies of aggregates of derivative **3** with trifluoroacetic acid

(TFA) which is strong non-aromatic acid, under same set of conditions as used for PA. The emission spectra show appearance of emission band at 439 nm upon addition of 1.5 μl of TFA (10⁻¹ M) which confirms the protonation of pyridyl nitrogen of aggregates of derivative **3** in excited state (Fig. S11 in ESI†). Interestingly, no significant quenching of emission band at 339 nm was observed. Thus the nature of interaction between aggregates of derivative **3** and PA is considerably different from that with other acidic molecules. Furthermore, the emission signal corresponding to protonated species is more red shifted in presence of PA (Δλ = 121 nm) (Figure 1C) as compared to that in presence of TFA (Δλ = 100 nm) (Fig. S11 in ESI†). We believe that in comparison to electron deficient and acidic PA, TFA has only acidic character and thus, different sensing response is observed. We recorded the absorption spectra of aggregates of derivative **3** in H₂O:EtOH (6:4) in the presence of TFA (Fig. S12 in ESI†). No new band corresponding to the protonated species was observed which also confirms that protonation of aggregates is an excited state phenomenon (Fig. S12 in ESI†). Further, we also carried out fluorescence titration of derivative **3** after protecting the hydroxyl group of PA with methoxy group (Fig. S13 in ESI†). Interestingly no new band appeared after protecting the phenolic hydroxyl group of PA with methoxy group. However, there is only quenching of emission band at 339 nm. These studies clearly indicate that the formation of emission band at 460 nm is due to excited state intermolecular proton transfer from PA to pyridyl nitrogen. To confirm that the protonation of aggregates of derivative **3** is not a ground state phenomenon, we studied the effect of triethylamine on emission spectra of aggregates of derivative **3** in presence of PA. The addition of 8 equiv of triethylamine (10⁻² M) results in gradual weakening of the band at 460 nm, however, emission band at 339 nm was not revived (Fig. S14 in ESI†). On the other hand, no significant change was observed in the absorption spectra of aggregates of derivative **3** in presence of PA with the addition of triethylamine (Fig. S15 in ESI†). These results further confirm that the protonation of aggregates of derivative **3** is an excited state phenomenon and the protonated species cannot be observed in the ground state. Further the SEM image of derivative **3** in H₂O:EtOH (6:4) in the presence of 7 equiv. of PA shows layered flakes, thus indicating modulation of self

assembled structure of derivative **3** on addition of PA {Figure 1B (ii)}.

Under same set of conditions as used for the detection of PA, we also carried out fluorescence studies of aggregates of derivative **3** in presence of NT (40 equiv), DNT (62 equiv), TNT (65 equiv), BQ (120 equiv) and NM (135 equiv), DNB (82 equiv) but no new band corresponding to the protonated species was observed (Fig. S16 in ESI†). Further, we also carried out fluorescence studies of aggregates of derivative **3** with phenolic derivatives (catechol, Br-phenol, I-phenol, 2,4-dinitrophenol (DN), 4-nitrophenol (NP) and phenol) but no new band appeared at 460 nm upon titrations with phenolic derivatives, however emission bands at 302 and 325 nm are the characteristic emission bands of phenol and catechol itself (Fig. S17 in ESI†). Thus, the derivative **3** is selective towards PA and ‘no quenching’ response is observed only in case of PA amongst various nitro derivatives and phenol derivatives tested (Fig. S18 in ESI†). The fluorescence life time studies of aggregates of derivative **3** monitored at 339 nm show shorter decay time (0.606 ns), however at 460 nm, in presence of PA (6 equiv) a long lived component (0.840 ns) is observed (Fig. S19 in ESI†). This result suggests the formation of a new fluorescent species due to interaction between derivative **3** and PA. The detection limit in this case was found to be 26 nM (Fig. S20 in ESI†). We also carried out pH studies and it is found that emission spectra of solution of derivative **3** in buffer:EtOH (6:4) mixture using universal buffer is independent of pH in the range of 6 to 14 (Figure 3A). Further, the effect of PA on derivative **3** at different pH values was also studied. At pH = 2 (acidic), the fluorescence spectra initially shows the emission band at 439 nm and with the addition of 16 equivs. (0.8 mM) PA the emission band at 439 nm shifted to longer wavelength and finally reaches to emission at 460 nm which corresponds to protonated species (Figure 3B). However at pH = 12 (basic), the effect of PA on derivative **3** is same as that at neutral pH = 7. At acidic pH = 2, more equivs. of PA are required for protonation because of already protonated pyridyl groups, which slows down the transfer of proton from PA to pyridyl nitrogen (Fig. S21 in ESI†).

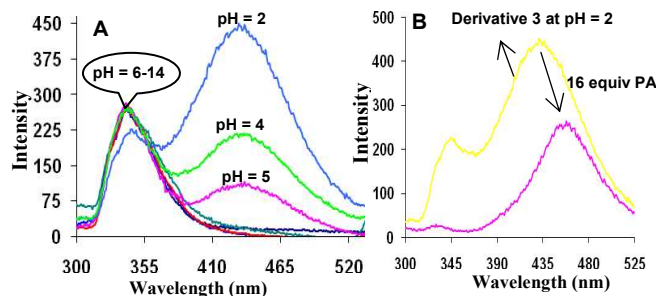


Figure 3. (A) Fluorescence emission spectra of derivative **3** (50 μM) at different pH scale in universal buffer:EtOH (6:4); $\lambda_{\text{exc}} = 273$ nm. (B) fluorescence emission spectra of derivative **3** (50 μM) at pH = 2 with the addition of 16 equivs (0.8 mM) of PA in H₂O:EtOH (6:4); $\lambda_{\text{exc}} = 273$ nm.

To study the role of 3-pyridyl/2-pyridyl groups in “no quenching” response, we recorded the fluorescence spectra of derivatives **4** and **5** in the presence of PA. Both the derivatives have rotors and form aggregates in aqueous media. Interestingly, solution of derivative **4** having 2-pyridyl groups in H₂O:EtOH (3:7) mixture exhibits “no quenching” response towards PA (Figure 4A) whereas under same set of conditions derivative **5** having 3-pyridyl groups exhibits quenching of emission in presence of PA (Figure 4B). No new band was observed in case of derivative **5** having 3-pyridyl group with the addition of PA which suggest the site of protonation is only in the 2-pyridyl groups. We also carried out fluorescence studies of derivative **5** in presence of TFA, however, no significant change in the emission spectra was observed (Fig. S22 in ESI†). The SEM image of derivative **5** shows the presence of spherical aggregates (Fig. S23 in ESI†). It is expected that 3-pyridyl nitrogens will be present at the periphery and may be hydrogen bonded to the solvent molecules. We believe that 3-pyridyl group has relatively weaker basicity not enough to enable the excited state proton transfer. These results suggest the importance of 2-pyridyl groups for “no quenching” detection of PA in aqueous media.

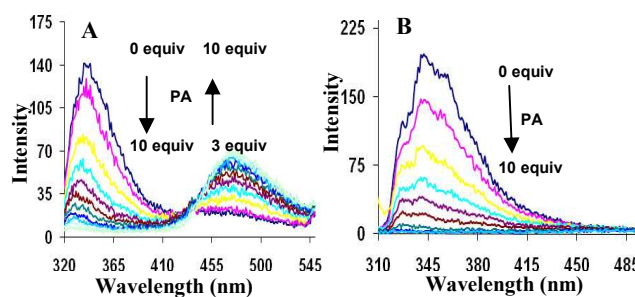


Figure 4. (A) Fluorescence emission spectra of derivative **4** (50 μM) with the addition of picric acid (500 μM) in H₂O:EtOH (3:7) buffered with HEPES pH = 7; $\lambda_{\text{exc}} = 273$ nm. (B) Fluorescence emission spectra of derivative **5** (5 μM) with the addition of Picric Acid in H₂O:EtOH (6:4) buffered with HEPES pH = 7; $\lambda_{\text{exc}} = 290$ nm.

Further, PA can contaminate the human body, clothing and other materials in the surroundings during manufacturing of rocket fuel and fireworks. Detection of these traces are major concern in field of analytical and forensic sciences. In this context, we prepared TLC strips by dip-coating solution of aggregates of **3** on TLC strips followed by drying it under vacuum for checking of residual contamination in contact mode. We prepared several samples of solution coated TLC strips and studied the response of their fluorescence towards picric acid in contact mode and solution phase. PA crystals were placed over a coated TLC strips for 5 sec. to test the contact mode response of nanoflakes of derivative **3** towards PA. Upon illumination with UV lamp, blue spots were observed in the contact area {Figure 5(i) (a-b)}. We also checked the effect of various concentrations of PA, DNT and TNT solution on the fluorescent TLC strips by applying small spots of different concentrations of analytes to the TLC strips {Figure 5(ii) (a-f)}. The minimum amount of PA detectable by the naked eye was as low as 10 μL of 1×10^{-12} M solution, thereby registering a detection limit of 2.29 femtogram level, whereas these TLC strips were not found to be sensitive towards DNT and TNT {Figure 5(ii) (a-f)}. However,

no visible quenching was observed by applying blank solvent (ethanol) on fluorescent paper strips {Figure 5(ii) a}.

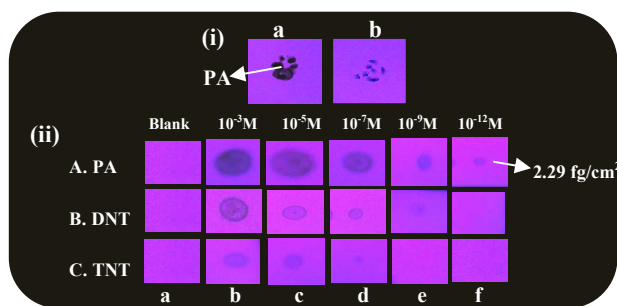


Figure 5. Photographs of derivative **3** coated TLC strips under different experimental conditions (i) (a) PA crystals on the top of derivative **3** coated TLC strips (b) removal of PA crystal after 5 secs. (ii) photographs of fluorescence quenching of derivative **3** coated TLC strips by PA, DNT and TNT on contact mode (10 μ l of analyte with the contact area of 0.05 cm²) when viewed under 365 nm UV illumination.

Conclusion

In conclusion, we designed and synthesized hetero-oligophenylene derivative **3** which forms fluorescent aggregates in aqueous media and these aggregates work as efficient and selective ‘no quenching’ fluorescent sensor for detection of picric acid in solution and solid state. In addition to this, we have prepared the fluorescent TLC strips carrying aggregates of derivatives **3** which can detect the PA up to femtogram level.

General Experimental methods

All the fluorescence spectra were recorded on SHIMADZU 5301 PC spectrofluorometer. UV spectra were recorded on Shimadzu UV-2450PC spectrophotometer with a quartz cuvette (path length: 1 cm). The cell holder was thermostated at 25 °C. Elemental analysis was done using a Flash EA 1112 CHNS/O analyzer of Thermo Electron Corporation. ¹H and ¹³C NMR spectra were recorded on JEOL-FT NMR-AL 300 MHz spectrophotometer and Bruker (Avance II) FT-NMR 400 MHz spectrophotometer using CDCl₃ and DMSO-d₆ as solvent and tetramethylsilane (Si(CH₃)₄) as internal standards. Data are reported as follows: chemical shifts in parts per million (δ), multiplicity (s = singlet, br = broad signal, d = doublet, m = multiplet), coupling constants (Hz), integration, and interpretation. All spectrophotometric titration curves were fitted with SPECFIT 32 software. All spectral characterizations were carried out in HPLC-grade solvents at 20 °C within a 10 mm quartz cell.

Fluorescence quantum yield: 9,10-diphenylanthracene ($\phi_f = 0.95$) in ethanol has been used as standard in the measurement of fluorescence quantum yield by using Equation (1), in which ϕ_{fs} is the radiative quantum yield of the sample, ϕ_{fr} the radiative quantum yield of the reference, A_s and A_r are the absorbance of the sample and the reference, respectively, D_s and

D_r the areas of emission for the sample and reference, L_s and L_r are the lengths of the absorption cells, and N_s and N_r are the refractive indices of the sample and reference solutions (pure solvents were assumed).

$$\phi_{fs} = \phi_{fr} \times \frac{1-10^{-A_r L_r}}{1-10^{-A_s L_s}} \times \frac{N_s^2}{N_r^2} \times \frac{D_s}{D_r}$$

Equation 1

Experimental Details of Finding the Detection Limit: To determine the detection limit, fluorescence titration of compound **3** with picric acid was carried out by adding aliquots of a picric acid solution of micromolar concentration and plotting the fluorescence intensity as a function of picric acid. From this graph, the concentration at which there was a sharp change in the fluorescence intensity multiplied with the concentration of receptor gave the detection limit.

Preparation of TLC Strips: TLC strips (5cm \times 2 cm) were prepared by coating with derivative **3** (50×10^{-6} M) followed by removal of solvent under vacuum at room temperature. The ensemble coated filter papers were then cut into 8 pieces (1 cm \times 1 cm) to get the test strips and used for the detection of explosives.

Contact Mode Visual Detection of PA: Aqueous samples were prepared by dissolving PA in EtOH. The explosive solutions were spotted onto the TLC strips at the desired concentration level using a micropipette. A solvent blank was spotted near to the spot of each explosive. In order to ensure consistent analysis, all depositions were prepared from a 10 μ L volume, thereby producing a spot of ~ 0.5 cm in diameter. After solvent evaporation, the filter paper was illuminated with 365 nm UV light. The blue coloured spots (under UV light) were identified by an independent observer, and each set of experiments was repeated three times for consistency. The detection limits were calculated from the lowest concentration of the explosive that enabled an independent observer to detect the quenching visually.

Experimental Details

The compound **1a**,²⁸ **2a**,²⁹ **1b**,³⁰ and **5²⁸** were synthesized according to literature procedure.

Synthesis of compound 3: A solution of 3-(2-(pyridin-3-yl)ethynyl)pyridine **1a**²⁸ (1.4 mmol) and 2,5-diphenyl-3,4-di(pyridin-2-yl) cyclopenta-2,4-dienone **2a**²⁹ (1.4 mmol) in diphenyl oxide (2 mL) was refluxed under an atmosphere of nitrogen. After 18 h, the reaction mixture was cooled to room temperature followed by the slow addition of hexane (5 mL) to the reaction mixture. The hexane was decanted off and the rest of the crude product was purified by column chromatography using CHCl₃:Hexane (8:2) as eluent to give a beige solid (70%); ¹H NMR (400 MHz, CDCl₃): δ = 8.16 [d, J = 4 Hz, 2H, ArH], 8.12 [d, J = 4 Hz, 2H, ArH], 8.08 [s, 2H, ArH], 7.24 [d, J = 4 Hz, 2H, ArH], 7.17 [d, J = 4 Hz, 2H, ArH], 7.02 [d, J = 4 Hz, 2H, ArH], 8.08 [s, 2H, ArH], 6.83-6.91 [m, 10H,

ArH], 6.8 [t, J = 4 Hz, 2H, ArH]; ^{13}C NMR (100 MHz, CDCl_3): 158.25, 151.55, 151.27, 147.88, 146.98, 140.87, 138.68, 138.31, 138.10, 137.79, 134.7, 130.86, 127.37, 127.04, 126.54, 126.19, 122.26, 120.66; ESI-MS: Calculated: 538.2157; Found: 539.2302 ($\text{M}+1$) $^+$; Elemental analysis: Calcd. for $\text{C}_{38}\text{H}_{26}\text{N}_4$: C 84.73; H 4.87; N 10.40; Found: C 84.41 %; H 4.72 %, N 10.15 %.

Synthesis of compound 4: A solution of 1,2-diphenylethylene **1b**³⁰ (1.4 mmol) and 2,5-diphenyl-3,4-di(pyridin-2-yl) cyclopenta-2,4-dienone **2a**²⁹ (1.4 mmol) in diphenyl oxide (2 mL) was refluxed under an atmosphere of nitrogen. After 18 h, the reaction mixture was cooled to room temperature followed by the slow addition of hexane (5 mL) to the reaction mixture. The hexane was decanted off and the rest of the crude product was purified by column chromatography using CHCl_3 :Hexane (8:2) as eluent to give a beige solid (65%); ^1H NMR (400 MHz, CDCl_3): δ = 8.13 [d, J = 4 Hz, 2H, ArH], 7.19 [t, J = 4 Hz, 2H, ArH], 6.98 [d, J = 4 Hz, 2H, ArH], 6.73-6.86 [m, 22H, ArH]; ^{13}C NMR (100 MHz, CDCl_3): 120.29, 125.37, 125.49, 126.63, 126.71, 131.14, 131.27, 134.44, 139.71, 140.12, 141.21, 147.66; ESI-MS: Calculated: 536.2252; Found: 537.2332 ($\text{M}+1$) $^+$; Elemental analysis: Calcd. for $\text{C}_{40}\text{H}_{28}\text{N}_2$: C 89.52; H 5.26; N 5.22; Found: C 89.31 %; H 5.01 %, N 5.11.

Acknowledgment

We are thankful to DST (ref. no. SR/S1/OC-63/2010 and SR/S1/OC-69/2012) and CSIR (ref. no. 02(0083)/12/EMR-II) for financial support. SK is thankful to “UGC-BSR” Scheme for providing fellowship.

Notes and references

Department of Chemistry, UGC-Centre for Advanced Studies-I, Guru Nanak Dev University, Amritsar, Punjab, India.

E-mail :vanmanan@yahoo.co.in; mksharmaa@yahoo.co.in

† Electronic Supplementary Information (ESI) available: Synthesis of compound **3** and **5**, characterization data, UV-vis and fluorescence studies. See DOI: 10.1039/b000000x/

1 Safety Data Sheet for Picric Acid, Resource of National Institute of Health.

2 P. C. Ashbrook and T. A. Houts, *ACS Div. Chem. Health Safety*, 2003, **10**, 27.

3 G. V. Perez and A. L. Perez, *J. Chem. Educ.*, 2000, **77**, 910.

4 R. L. Woodfin, Trace Chemical Sensing of Explosives; John Wiley & Sons Inc.: Hoboken, NJ, 2007.

5 J. Shen, J. Zhang, Y. Zuo, L. Wang, X. Sun, J. Li, W. Han and R. He, *J. Hazard. Mater.*, 2009, **163**, 1199.

6 D. T. Meredith and C. O. Lee, *J. Am. Pharm. Assoc.*, 1939, **28**, 369.

7 E. H. Volwiler, *Ind. Eng. Chem.*, 1926, **18**, 1336.

8 J. Akhavan, *Chemistry of Explosives*, 2nd ed.; Royal Society of Chemistry: London, 2004.

9 P. Cooper, *Explosive Engineering*; Wiley-VCH: New York, 1996; p33.

10 X. Yang, C. J. Niu, G. L. Shen and R. Q. Yu, *Analyst*, 2001, **126**, 349.

11 C. Jian and W. J. Seit, *Anal. Chim. Acta.*, 1990, **237**, 265.

12 S. J. Toal and W. J. Trogler, *J. Mater. Chem.*, 2006, **16**, 2871.

13 D. Li, J. Liu, R. T. K. Kwok, Z. Liang, B. Z. Tang and J. Yu, *Chem. Commun.*, 2012, **48**, 7167.

14 S. Shanmugaraju, H. Jadhav, Y. P. Patil and P. S. Mukherjee, *Inorg. Chem.*, 2012, **51**, 13072.

15 L. Ding, Y. Liu, Y. Cao, L. Wang, Y. Xin and Y. Fang, *J. Mater. Chem.*, 2012, **22**, 11574.

16 S. S. Nagarkar, B. Joarder, A. K. Chaudhari, S. Mukherjee and S. K. Ghosh, *Angew. Chem. Int. Ed.*, 2013, **52**, 2881.

17 J. D. Xiao, L. G. Qiu, F. Ke, Y. P. Yuan, G. S. Xu, Y. M. Wang and X. Jiang, *J. Mater. Chem. A*, 2013, **1**, 8745.

18 S. Kumar, N. Venkatramaiah and S. Patil, *J. Phys. Chem. C*, 2013, **117**, 7236.

19 B. Roy, A. K. Bar, B. Gole and P. S. Mukherjee, *J. Org. Chem.*, 2013, **78**, 1306.

20 N. Venkatramaiah, S. Kumar and S. Patil, *Chem. Commun.*, 2012, **48**, 5007.

21 T. Liu, L. Ding, G. He, Y. Yang, W. Wang and Y. Fang, *ACS Appl. Mater. Interfaces*, 2011, **3**, 1245.

22 M. E. Germain, M. J. Knapp, *J. Am. Chem. Soc.* 2008, **130**, 5422.

23 A. Barba-Bon, A. M. Costero, S. Gil, M. Parra, J. Soto, R. Martinez-Manez, F. Sancenon, *Chem. Commun.*, 2012, **48**, 3000.

24 Y. Xu, B. Li, W. Li, J. Zhao, S. Sun and Y. Pang, *Chem. Commun.*, 2013, **49**, 4764.

25 J. C. Sanchez and W. C. Trogler, *J. Mater. Chem.*, 2008, **18**, 3143.

26 M. Irie, T. Fukaminato, T. Sasaki, N. Tamai and T. Kawai, *Nature*, 2002, **420**, 759.

27 For comparison with reported PA sensors, See Electronic Supplementary Information, Table S1, page S21.

28 V. Bhalla, V. Vij, A. Dhir and M. Kumar, *Chem.-Eur. J.*, 2012, **18**, 3765.

29 Z. Li, L. Zhang, L. Wang, Y. Guo, L. Cai, M. Yu and L. Wei, *Chem. Commun.*, 2011, **47**, 5798.

30 M. J. Mio, L. C. Kopel, J. B. Braun, T. L. Gadzikwa, K. L. Hull, R. G. Brisbois, C. J. Markworth and P. A. Grieco, *Org. Lett.*, 2002, **4**, 3199.

31 L. Zhao, R. Ma, J. Li, Y. Li, Y. An and L. Shi, *Biomacromolecules*, 2008, **9**, 2601.

32 H. Yao, K. Domoto, T. Isohashi, K. Kimura, Langmuir, 2005, **21**, 1067.

33 I. Struganova, *J. Phys. Chem. A*, 2000, **104**, 9670.

34 K. R. Wang, D. S. Guo, B. P. Jiang, Z. H. Sun, and Y. Liu, *J. Phys. Chem. B*, 2010, **114**, 101.

35 J. N. Demas and G. A. Grosby, *J. Phys. Chem.* 1971, **75**, 991.

36 J. Herbich, C. Y. Hung, R. P. Thummel and J. Waluk, *J. Am. Chem. Soc.*, 1996, **118**, 3508.

37 H. Berber, C. Ogretir, E. C. S. Lekesiz and E. Ermis, *J. Chem. Eng. Data* 2008, **53**, 1049.

38 J. R. Albani, Principles and Applications of Fluorescence spectroscopy; Blackwell Science, 2007, P 79-87.

39 I. M. Kolthoff and M. K. Chantooni, Jr. *J. Am. Chem. Soc.* 1965, **87**, 4428.

